

High strain rate of quartz glass and its effects during high-speed dicing

Kenan Li^{a,b}, Yangwei Wang^c, Yanjun Zhao^b, Chenxia Jin^d, Hu Tang^e, Qin Zou^a, Yucheng Zhao^a, Mingzhi Wang^{a,*}

^a State Key Laboratory of Metastable Materials Science and Technology, College of Material Science and Engineering, Yanshan University, Qinhuangdao, 066004, China

^b State Key Laboratory of Superabrasives, Zhengzhou Research Institute for Abrasive & Grinding Co. Ltd., Zhengzhou, 450001, China

^c Beijing Institute of Technology, Beijing, 100081, China

^d Zhengzhou Bus Communication Corporation, Zhengzhou, 450007, China

^e Center for High Pressure Science & Technology Advanced Research, Beijing, 100094, China



HPSTAR
767-2019

ARTICLE INFO

Keywords:

High-speed dicing
High strain rate
Diamond dicing blade
Quartz glass

ABSTRACT

Strain rate is a key parameter that affects dynamic mechanical properties of materials in a high-speed crash. It is equally important in the materials processing field. In this study, we investigate the high strain rate of quartz glass and its effects during the high-speed dicing with diamond blades. A formula is derived to predict the strain rates of quartz glass at different linear velocities of diamond blades. High-speed crashing and dicing tests are performed to verify the formula and explore the effects of high strain rate by using the split Hopkinson pressure bar test and an automatic high-speed dicing saw. Results indicate that strain rate increases as the linear velocity of a diamond dicing blade increases. High strain rate results in hardening effects and heat generation for quartz glass. The dicing temperature is at least 1043 °C because of the generated silicon and graphite in the dicing area. The theory of high strain rate reveals the wear mechanism of diamonds, and indicates that the dicing speed for quartz glass should not be more than 60.71 mm/s. This research expands the study of dynamic hardness to the high-speed grinding field. The study helps design diamond tools and optimize the parameters of machining materials.

1. Introduction

Quartz glass is widely used in optics, optical communication and other fields in view of its optical and mechanical performance. It consists of a number of Si-O tetrahedrons (Fig. 1), one of which is composed with one silicon atom and four oxygen atoms [1]. However, it is difficult to be machined due to its higher hardness and brittleness [2]. It is prone to brittle fracture, cracking, overload and other defects during the high-speed dicing process. Because of its higher hardness, diamond particles can be used to machine many materials, such as quartz glass [3]. The common diamond tools included diamond dicing blades, diamond wheels, diamond grinding disc and so on [4]. So far, the wear mechanism of diamond tools and grinding progress have been studied by many researchers. Shang et al. studied the mechanisms of edge chipping on the basis of machining mechanics and energy theories [5]. Inasaki suggested that high machining speed was needed for hard and brittle materials [6]. Koji found that the cutting ability of dicing blades was depended on the fresh diamonds [7]. Previous researches focused on the wear mechanism and grinding process, but few studies of strain rate and its effects have been conducted in materials processing field.

Strain rate is a key parameter that affects flow stress and dynamic hardness of materials [8–10]. In defensive and military fields, there are many investigations conducted on high strain rates, which mainly have been adopted by a split Hopkinson pressure bar (SHPB) test (Fig. 2). Previous studies indicated that there was some relevance among dynamic hardness, flow stress, and strain rate [11,12]. Y.F Zhang et al. showed that the hardness and elastic modulus of enamel grew with strain rate increase [13]. Hana Jung Jitang Fan et al. investigated the compressive mechanical response of strain rates with SHPB test [14,15]. Chaudhri and Luke A et al. argued that the dynamic hardness of materials was different from that of quasi-static under high strain rate [16,17]. Amin et al. believed that hardness of materials depended on strain rate with micromechanical models [18]. Weiliang Zhang et al. found that fracture developed due to the combination of shear and ductile failure under higher strain rates [19]. Nathan et al. found that high shear strain rates generated high temperatures in the shear plane of a specimen [20]. The above studies of strain rates mainly focused on the field of national defense. There are few studies of strain rates that have been conducted in materials processing field.

As a brittle material, quartz glass is removed by means of impact

* Corresponding author.

E-mail address: 18236799001@163.com (M. Wang).

<https://doi.org/10.1016/j.ceramint.2019.04.057>

Received 25 December 2018; Received in revised form 4 April 2019; Accepted 6 April 2019

Available online 08 April 2019

0272-8842/ © 2019 Elsevier Ltd and Techna Group S.r.l. All rights reserved.

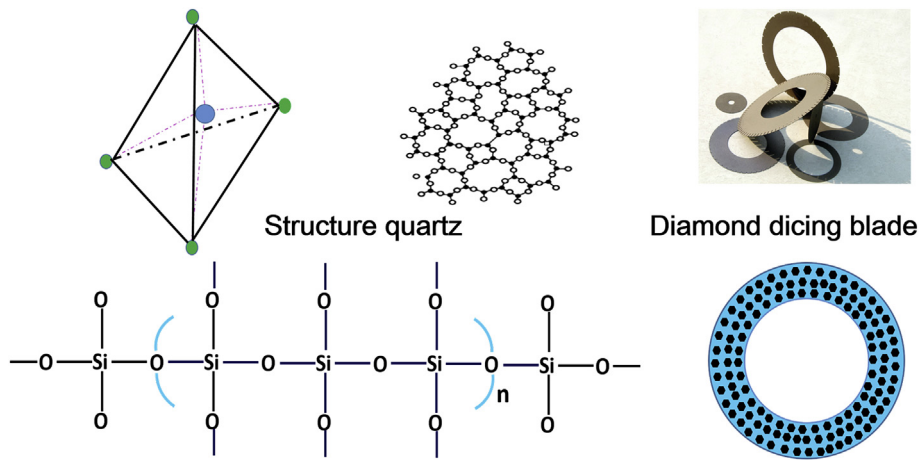


Fig. 1. Microstructures of quartz glass and diamond dicing blades.

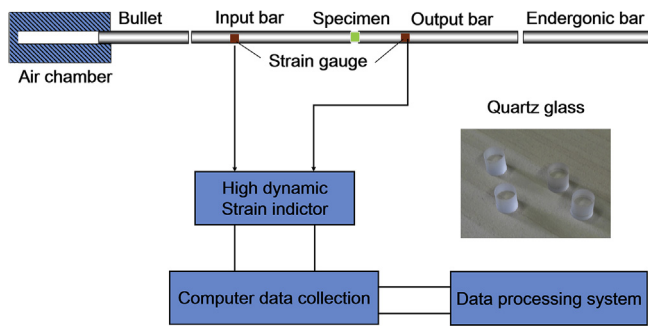


Fig. 2. Diagram of SHPB system.

with diamonds. The impacting time is quite short due to the high speed of revolving diamond blades. This paper focuses on the high strain rate of quartz glass during a high-speed dicing process with diamond dicing blades. We derive a formula of strain rate on the basis of grinding and strain theories. Then, we carry out high-speed crashing and dicing tests to verify the formula and explore the effects of high strain rate by using SHPB test and automatic high-speed dicing saw. Furthermore, we examine high-strain-rate effects, including the hardening and generating heat of quartz glass with Raman spectroscopy and scanning electron microscopy. The study reveals the wear mechanism of diamonds and optimizes the parameters of machining quartz glass.

2. Materials and methods

2.1. Experimental materials

Diamond dicing blades with ϕ 40 mm in inner diameter and ϕ 58 mm in outer diameter were used to conduct dicing tests. These blades are of the same thickness (300 μ m) and uniform diamond grain size (30 ~ 50 μ m). The matrix material of diamond dicing blades was bronze bond. The outer diameter of flanges was ϕ 49.6 mm. The exposure length of diamond dicing blades in the initial condition was 4.2 mm. Two kinds of specifications of quartz glass were considered for testing: 30 mm (w) \times 2 mm (h) \times 100 mm (l) for the dicing test and ϕ 5 mm \times 5 mm for the SHPB test. Stainless steel and common glass shared a common specification, i.e., 30 mm (w) \times 2 mm (h) \times 100 mm (l).

2.2. Experimental methods

A series of dicing tests were performed on DISCO DAD 3350 automatic dicing saw under designed dicing conditions. The curves of strain–stress under different strain rates were measured through SHPB tests. The quasi-static behavior of quartz glass was carried out on the WDW-100EB materials testing machine. The interfacial reactions between quartz glass and diamonds were proved with the Raman microscope INVIA. The wear morphologies of diamonds under different rotational speeds were observed with the scanning electron micrograph S-4800.

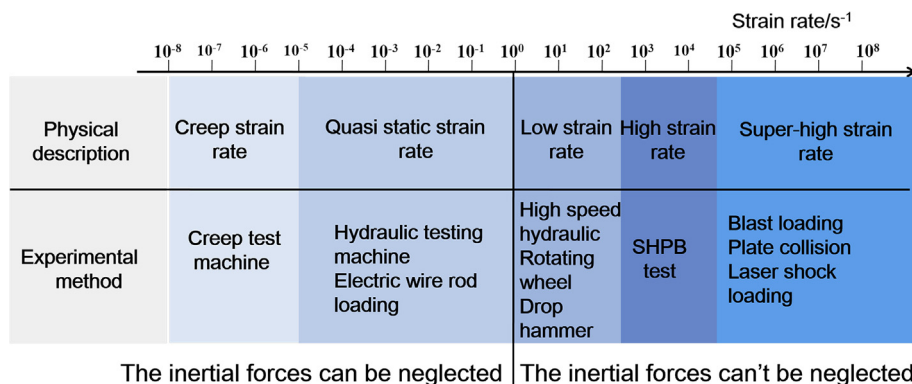


Fig. 3. Classification of stain rates.

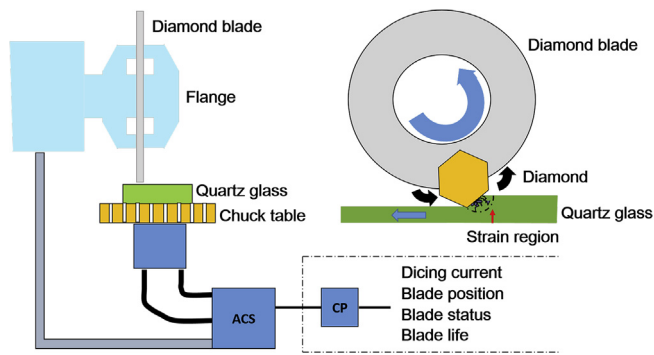


Fig. 4. The diagram of a diamond crashing into quartz glass at high speed.

3. Theory and calculation

3.1. Calculations for strain rates of quartz glass in high-speed dicing

According to the magnitude of strain rates, we can classify them into creep, quasi-static, low, high, and super-high strain rates [21,22], as shown in Fig. 3. The rotational speed of an automatic dicing saw reaches up to 60,000 rpm. As a hard and brittle material, quartz glass is removed by means of impact with diamonds. Fig. 4 shows the diagram of a diamond crashing into quartz glass at high speed, in which ACS is Active Control System, CP is Characteristic Parameter. Plenty of diamonds and binding agent make up a diamond dicing blade. When a diamond blade is rotating at high speed, countless crashes occur at high strain rate. Nevertheless, there are few formulas to predict the strain rate of quartz glass during high-speed dicing. It is in urgent need of a unified formula to calculate the strain rate of quartz glass under different linear velocities of wheels in the high-speed grinding field.

The focus of our work is on the variation of strain rate against dicing speed during a high-speed dicing process. The thickness of a dicing blade is generally between 0.1 mm and 0.3 mm, and the rotating speed of a dicing blade is usually between 30000 rpm and 60000 rpm. There are plenty of diamonds and binder in a dicing blade. If every diamond and binder of a dicing blade is all considered, the calculated amounts is huge. The elastic deformation is related to the contact surface of workpieces. We make these assumptions to simplify the calculation of strain rates and concentrate the research. On the basis of previous studies [17,18], we made three assumptions to predigest the calculation.

Three assumptions are made to obtain the formula for the strain rate of quartz glass in high-speed dicing. First, the thickness of a diamond dicing blade is approximately equal to the diameter of a diamond, and this blade is homogeneous. Second, the length of deformation is approximately equal to the contact arc length of materials removal region. Third, elastic strain and crushing phases exist when a metal-bonded diamond blade is dicing quartz glass at a high speed. A high strain rate is generated in the elastic strain phase, and the destruction occurs in the crushing phase.

According to Hooke's law, strain (ϵ) can be calculated as Eq. (1). Strain rate ($\dot{\epsilon}$) is obtained by Eq. (2), where E_q is the elasticity modulus of quartz glass, t is the duration time of strain, and σ is the stress of quartz glass in high-speed dicing with a diamond dicing blade.

$$\epsilon = \frac{\sigma}{E_q} \quad (1)$$

$$\dot{\epsilon} = \frac{\epsilon}{t} = \frac{\sigma}{E_q \cdot t} \quad (2)$$

In a high-speed dicing or grinding process, the inertial force that is called centrifugal force (f) cannot be neglected. It can be obtained by using Eq. (3), where ρ_w and D_w are the density and diameter of a diamond dicing blade, respectively. v_s is the linear velocity of a diamond

dicing blade, and v_w is the velocity of a workbench.

$$f = \frac{2 \cdot \rho_w \cdot (v_s + v_w)^2}{D_w} \quad (3)$$

Combining Eq. (3), we can get Eq. (4). The contact arc length (l_c) of the material removal region can be calculated as Eq. (5), where D_w is the diameter of a diamond dicing blade and d_p is the dicing depth [23].

$$\sigma = \frac{f}{s} = \frac{8 \cdot \rho_w \cdot (v_s + v_w)^2}{\pi \cdot D_w^3} \quad (4)$$

$$l_c = \sqrt{D_w \cdot d_p} \quad (5)$$

$$t = \frac{l_c}{v_s + v_w} = \frac{\sqrt{D_w \cdot d_p}}{v_s + v_w} \quad (6)$$

By substituting Eqs. (4) and (6) into Eq. (2), we obtain the formula of the strain rate of quartz glass at different crashing speeds, as shown in Eq. (7), where v_s can be calculated with Eq. (8) in which n is the rotational speed of a spindle.

$$\dot{\epsilon} = \frac{8 \cdot \rho_w \cdot (v_s + v_w)^3}{\pi \cdot D_w^3 \cdot E_q \cdot \sqrt{D_w \cdot d_p}} \quad (7)$$

$$v_s = \frac{\pi \cdot n \cdot D_w}{60000} \quad (8)$$

According to Eq. (7), the strain rate of quartz glass is related to linear velocity, feeding speed, diameter, dicing depth, density of a diamond blade, and elastic modulus of quartz glass. From Eq. (7), we obtain the curves of strain rate against linear velocity under different outer diameters of diamond blades. Fig. 5 illustrates that the strain rate of quartz glass grows as the velocity of a diamond dicing blade increases but decreases as the outer diameter of a diamond blade increases. A sharp increase occurs after reaching the linear velocity of 60.71 m/s. We also get the curves of strain rate against linear velocity at different dicing depths from Eq. (7). Moreover, the strain rate of quartz glass decreases as the dicing depth increases. During high-speed dicing or grinding, the strain rate of quartz glass increases up to $6.65 \times 10^5/s$ when a diamond dicing blade is dicing quartz glass at the linear velocity of 151.77 m/s (50000 rpm for a diamond dicing blade with $\phi 58mm$ in outer diameter). Hence, the effects of high strain rate on the dicing performance should not be neglected during high-speed dicing. According to the calculation of Eq. (7), the inflection point of strain rate in Fig. 5 is about 60 m/s, which is consistent with that of the dicing current in Fig. 8(b). High speed brings about high strain rate which leads to hardening and generating heat of materials. Under high strain rate, hardening of quartz glass and generated heat accelerate the wear of diamonds and increase the dicing load.

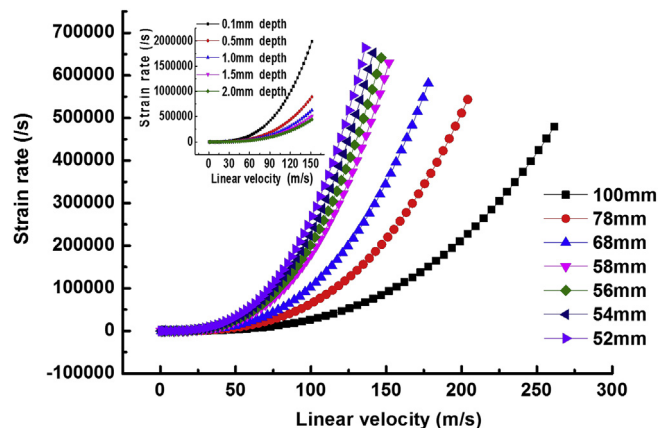


Fig. 5. Strain rates of quartz glass at different linear velocities.

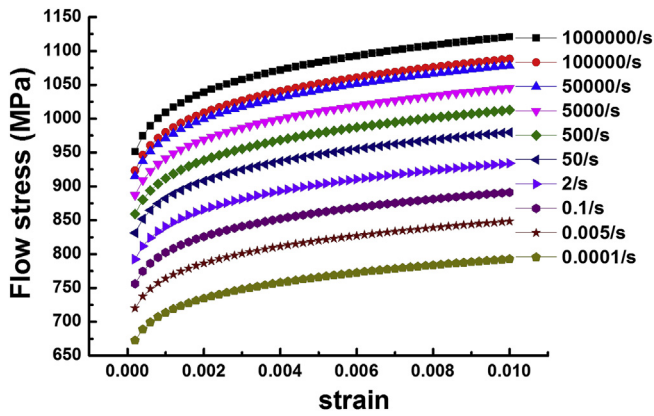


Fig. 6. Flow curves of strain-stress of quartz glass.

3.2. Theoretical curves of stress–strain under different strain rates

The yield limit of materials at a certain deformation temperature, strain, and strain rate is called flow stress. Eq. (9) shows that the constitutive equations express the relationship among stress and strain, temperature, strain rate, and other physical quantities [10]. The flow stress of materials under different strains, strain rates, and temperatures provides enough basic data for the numerical simulation of plastic deformation process for machining and impact analysis [24,25].

$$\sigma = f(\epsilon, \dot{\epsilon}, T) \tag{9}$$

There are several kinds of constitutive equations, and the Johnson–Cook (J–C) model is one of the most widely used constitutive models because of its fewer parameters and much simpler expressions relative to other available models [26–28]. For simplicity, the thermal softening factor (T) is not considered. This model also expresses the dynamic mechanical behavior and quasi-static deformation of materials over a wide range of strain rates. According to the J–C model, flow stress expression is revealed as follows: Eq. (10) [29], where σ is the dynamic flow stress; A is the yield stress at a given reference strain rate ($\dot{\epsilon}_0$), which is $0.0001s^{-1}$; ϵ denotes the plastic strain; B is the coefficient of strain hardening; C is the hardening coefficient of strain rate; n is the strain hardening exponent. The values are obtained from the SHPB tests and WDW-100EB materials tests of quartz glass by the method of fitting curve. According to Eq. (10), high strain rate results in increase of flow stress. Fig. 6 shows that the flow stress grows as strain rates increase.

$$\sigma = (A + B\epsilon^n) \cdot \left(1 + C \ln\left(\frac{\dot{\epsilon}}{\dot{\epsilon}_0}\right) \right) \tag{10}$$

$$Hv = 0.927\sigma_f C \tag{11}$$

The Vickers hardness of materials can be obtained by Eq. (11),

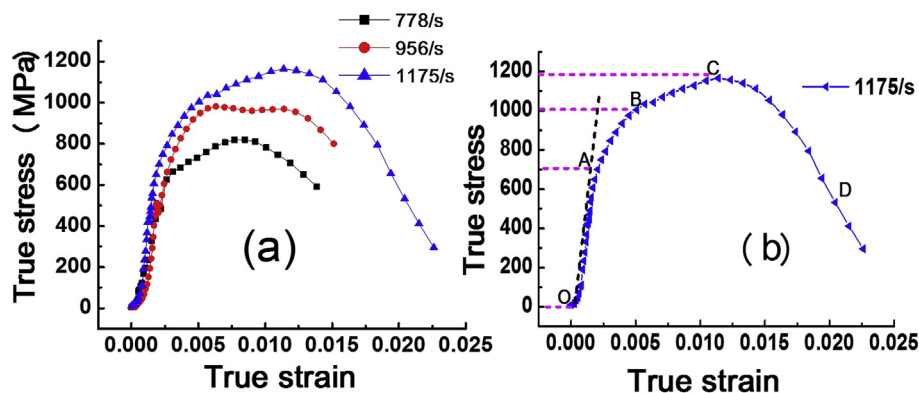


Fig. 7. Curves of strain-stress of quartz glass with SHPB test.

where C is the constraint factor and σ_f is the flow stress [30]. Hardness grows as flow stress increases. As a hard and brittle material, quartz glass is removed by means of impact with diamonds. When a diamond glass blade is rotating at a high speed, countless crashes occur at high strain rate. According to theoretical formulas Eq. (10) and Eq. (11), high strain rate improves the hardness of quartz glass during a high-speed dicing process.

4. Results and discussion

4.1. Hardening effect of quartz glass under high strain rates

Strain rate is one of the key parameters that determine flow stress [31,32]. Curves of strain-stress of quartz glass tested by SHPB is shown in Fig. 7(a). It shows that the true stress grows as strain rates increase. High strain rate leads to changes of material properties, which is different from that of static condition. Fig. 7(b) illustrates that the crashing process is divided into four stages: (1) elastic deformation stage (OA), (2) stable development stage of micro-cracks (AB), (3) unstable development stage of micro-cracks (BC), and (4) damage stage (CD). The stages of AB, BC and CD can be thought of a big phase which is called crushing phase. Under this phase, quartz glass begins to break into pieces. Stress, strain and strain rate are fundamental concepts for dislocation dynamics and macroscopic dynamics. The yield stress grows with the increase of strain rate, as shown in Fig. 7(a). Higher strain rate causes dislocation pile-up which prevent micro-cracks from generating and propagating, then prolongs material's fatigue life and improves the performance of materials.

Cracks propagation is the key factor affecting the dynamic hardness for the brittle materials. If the speed of crack propagation is lower than strain rate, generating and growing cracks are no longer necessary. Therefore, higher dynamic hardness becomes evident. Hardness of materials reflects the resistance to deformation under an applied load. Quartz glass is impossible to scratch a diamond under quasi-static or low strain rate. However, it will leave scratches on the surface of diamonds under high strain rate, as seen in Fig. 8(d) and (c). The results implies that there are different performances of materials under different strain rates due to the evolution of microstructures.

From macroscopic dynamics, under high strain rate, dynamic hardness (H_d) is different from that of quasi-static. Dynamic hardness depends on the strain rate of materials, as seen from Eq. (12), where K and q are the material constants of quartz glass, H_d is the dynamic hardness, $\dot{\epsilon}$ is the strain rate, and q is the creep rate sensitivity [13]. Eq. (12) suggests that the dynamic hardness of quartz glass grows as linear velocity increases, thereby accelerating the wear of diamonds.

$$H_d = K \cdot \dot{\epsilon}^q \tag{12}$$

Dicing current is one of the crucial parameters that can judge the wearing state of diamonds. When the edges of diamonds are wore out,

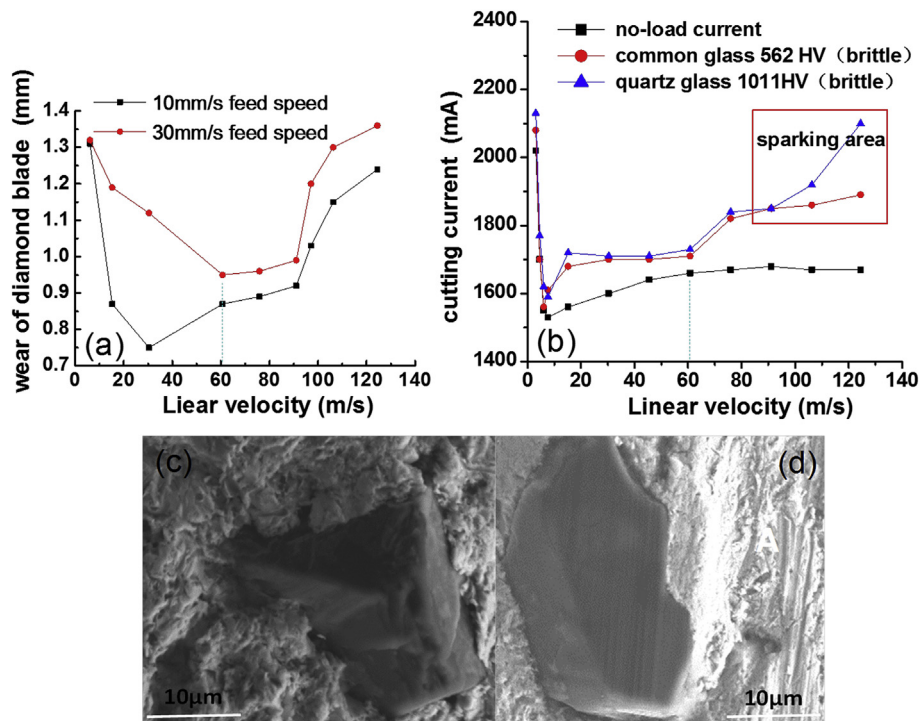


Fig. 8. The dicing load and wear morphology of a diamond blade.

the dicing current increases. Fig. 8(a) reveals that an exorbitantly high linear velocity exacerbates the wear of a diamond blade. Fig. 8(b) shows the trend of dicing current against linear velocity. The dicing current at first decreases as linear velocity increases, then increases from the linear velocity of 7.59 m/s and sharply rises from that of 60.71 m/s (20000 rpm for the diamond dicing blade with ϕ 58 mm in outer diameter).

Most people perceived that high speed brings about high efficiency in the materials processing field, and it was a popular method to increase the machining speed for most of materials. However, according to the investigation of high strain rates in this research, dicing speed is limited for the dicing of hard materials, such as quartz glass. High speed brings about high strain rates which lead to hardening and generating heat of materials. Fig. 8 illustrates that the linear velocity of 60.71 mm/s should not be exceeded, which is consistent with the strain rate curve of quartz glass in Fig. 5.

4.2. Generated heat effect of quartz glass at high strain rates

During a high-speed dicing process, the strain rate is so high that the increased hardness cannot neutralize the kinetic energy, then some of kinetic energy will transform into heat [19]. High strain rates lead to intensive bonding strength. It is difficult to expose fresh diamonds when passivated diamonds are in escalation. Passivated diamonds cannot effectively remove quartz glass only can generate plenty of heat. Meanwhile the crashing time is so short that the high-speed process is similar to be adiabatic.

Therefore, the temperature between quartz glass and diamond blades will significantly rise as strain rate increases. The value can be as high as hundreds of degrees Celsius. If this part of heat does not quickly dissipate, diamonds can be burned, and blades may be deformed. Meanwhile, if high strains do not match with heat transfer rates, systematic temperature will also rise and bring about negative effects on dicing behavior, such as deformation, graphitization, and spark, as shown in Fig. 8(b). Fig. 9 displays a spark area where a diamond blade is sparking and it is burned at a high rotational speed. There is plenty of heat if the strain rate is too high. The heat conductivity coefficient of

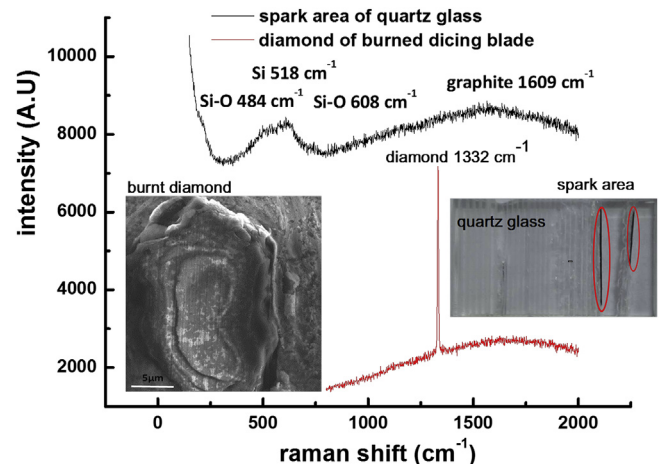


Fig. 9. The Raman shift of quartz glass in sparking area and burned diamonds.

quartz glass is low, whereas diamonds and metal binders have good conductivity of heat. Diamond dicing blades absorb such much heat that blades are burned, as shown in Fig. 9. This accelerates the wear of diamond dicing blades.

There is mechanochemical wear due to high dicing temperature under high strain rate. Eqs. (13)–(15) are primary chemical reactions if there is enough heat. To study the heat generated by high strain rates during a high-speed dicing process, we exploit the thermodynamic principle and Raman shift, as shown in Fig. 9. Standard Gibbs function, standard entropy, and standard enthalpy is derived too. The Gibbs functions of Eqs. (16)–(18) are formulated by exterior differential derived from the second law of thermodynamics. From these equations, we get the values of enthalpy, Gibbs energy, and entropy.

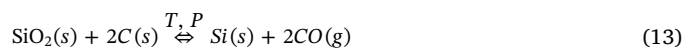


Table 1
The thermodynamic parameters of simple substances and compounds.

matters	$\Delta_f H_{m,T}^\ominus$	$\Delta_f G_{m,T}^\ominus$	$S_{m,T}^\ominus$
	KJ.mol ⁻¹	KJ.mol ⁻¹	K.mol ⁻¹ .K ⁻¹
C diamond	1.896	2.9	2.439
C graphite	0	0	5.694
Si	0	0	18.8
SiO ₂	-910.7	-856.3	41.5
CO	-110.5	-137.2	197.7
O₂	0	0	205.138

$$C_{(diamond)} \xrightleftharpoons[T, P]{} C_{(graphite)} \quad (15)$$

For Eq. (13), combined with Eqs. (16) and (17), we achieve the values of Gibbs energy and the lowest reacted temperature of 1591 °C. Table 1 presents the thermodynamic parameters of simple substances and compounds.

$$\Delta_f G_{m,T}^\ominus = \Delta_f H_{m,T}^\ominus - T\Delta_f S_{m,T}^\ominus \quad (16)$$

$$\Delta_f G_{m,T}^\ominus \approx \Delta_f H_{m,298.15}^\ominus - T\Delta_f S_{m,298.15}^\ominus \quad (17)$$

$$\Delta_f H_{m,298.15}^\ominus = [(-110.5 \times 2) + 0] - [-910.7 + 2 \times 1.896] \times 10^3$$

$$\Delta_f S_{m,298.15}^\ominus = (2 \times 197.7 + 18.8) - (2 \times 2.439 + 41.5)$$

$$\Delta_f G_{m,T}^\ominus = 685.908 \times 10^3 - T367.822$$

$$T = 1864 \text{ K} = 1591^\circ\text{C}$$

However, the partial pressure of CO is decreased as linear velocity increases. As shown in Eqs. (18)–(20), if the partial pressure of CO is 0.01 KPa, then the lowest reacting temperature can decrease to 1043 °C. As the lowest reacting temperature decreases, the wear of diamonds will be aggravated. Fig. 9 further validates the deduction.

$$\Delta_f G_{m,T} = \Delta_f G_{m,T}^\ominus + RT \ln Q \quad (18)$$

$$\Delta_f G_{m,T} = \Delta_f G_{m,T}^\ominus + RT \ln \left(\frac{P_{CO}}{P^\ominus} \right)^2 \quad (19)$$

$$\Delta_f G_{m,T} = \Delta_f H_{m,T}^\ominus - T\Delta_f S_{m,T}^\ominus + RT \ln \left(\frac{P_{CO}}{P^\ominus} \right)^2 \quad (20)$$

$$\Delta_f G_{m,T} = 685.908 \times 10^3 - T367.822 + 8.314T \ln \left(\frac{0.01}{101.325} \right)^2$$

$$T = 1316 \text{ K} = 1043^\circ\text{C}$$

Diamonds usually react with oxygen at first if plenty of oxygen is available. The generated graphite indicates that oxygen hardly exists around a diamond dicing blade. Fig. 9 shows that silicon and graphite are generated at the sparking area of quartz glass on the basis of the Si-Si Raman shift at 518 cm⁻¹ and graphite Raman shift at 1609 cm⁻¹. The peak of 484 cm⁻¹ is the quaternary silicon oxygen Raman shift, whereas the peak of 608 cm⁻¹ is the ternary silicon oxygen Raman shift. The peak of 1332 cm⁻¹ is the Raman shift of diamonds. Eq. (13) indicates that silicon dioxide does not chemically react with diamonds if the temperature is below 1591 °C at 101 KPa partial pressure or below 1043 °C at 0.01 KPa partial pressure. Generated silicon indicates that the dicing temperature between diamonds and quartz glass goes up to 1591 °C at 101 KPa partial pressure or 1043 °C at 0.01 KPa partial pressure. This chemical reaction also implies that the temperature between a diamond and quartz glass is at least 1043 °C. High strain rates can also bring about plenty of heat which can accelerate chemical interface reactions during high-speed dicing. The chemical interface reactions can further accelerate the wear of diamonds. The high strain rate of quartz glass leads to hardening of quartz glass and heat

generation, both of which accelerate the wear of diamonds during high-speed dicing.

5. Conclusions

In this research, we study the high strain rate of quartz glass and its effect during high-speed dicing with a diamond blade by using SHPB tests and an automatic high-speed dicing saw. The conclusions can be drawn as follows:

- (1) We derive a formula of strain rate at different crashing linear velocities of diamond blades. This rate increases up to $6.65 \times 10^5 \text{ s}^{-1}$ at 151.77 m/s.
- (2) The theoretical and experimental results indicate that the strain rate of quartz glass increases with the increase of the linear velocity of a diamond blade.
- (3) High speed brings about high strain rates that cause hardening of quartz glass and heat generation. The dicing temperature under high strain rate is at least 1043 °C because of the generated silicon and graphite in the dicing area.
- (4) On the basis of the theories of dynamic hardness and high strain rate, we reveal the wearing mechanism of diamonds at high speed dicing of quartz glass. Under high strain rate, hardening of quartz glass and generated heat accelerate the wear of diamonds and increase the dicing load. Moreover, the dicing speed of quartz glass, should not be exceed 60.71 mm/s.

Acknowledges

This project is sponsored by the Natural Science Foundation of Hebei Province of China (E2016203425) and the Key Projects of Scientific and Technological Research in Hebei Province (ZD2017074). This work is supported by Zhengzhou Research Institute for Abrasives & grinding Co. LTD, Yanshan University and Beijing Institute of Technology. Thanks for the help.

References

- [1] J. Wang, Z. Jia, Y.B. Guo, Shape-cutting of quartz glass by spark discharge-assisted diamond wire sawing, *J. Manuf. Process.* 34 (2018) [131]–[139] <https://doi.org/10.1016/j.jmapro.2018.06.001>.
- [2] J. Partyka, M. Gajek, K. Gasek, Effects of quartz glass grain size distribution on the structure of porcelain glaze, *Ceram. Int.* 40 (2014) 12045–12053 <https://doi.org/10.1016/j.ceramint.2014.04.044>.
- [3] James C. Sung, Michael Sung, The brazing of diamond, *J. Refract. Metals Hard Mater.* 27 (2009) 382–393 <https://doi.org/10.1016/j.jrmhm.2008.11.011>.
- [4] Bo Jiang, Jian Yun Shen, Xi Peng Xu, Study on force characteristics for high speed sawing of quartz glass with diamond blade, *Mater. Sci. Forum* 800 (2014) [144]–[149] <https://doi.org/10.4028/www.scientific.net/MSF.800-801.144>.
- [5] Shang Gao, Renke Kang, Zhigang Dong, Edge chipping of silicon wafers in diamond grinding, *Int. J. Mach. Tool Manuf.* 64 (2013) [31]–[37] <https://doi.org/10.1016/j.ijmactools.2012.08.002>.
- [6] I. Inasaki, Grinding of hard and brittle materials, *CIRP Ann. - Manuf. Technol.* 36 (1987) 463–471 [https://doi.org/10.1016/S0007-8506\(07\)60748-3](https://doi.org/10.1016/S0007-8506(07)60748-3).
- [7] Koji Matsumaru, A. Takata, K. Ishizaki, Advanced thin dicing blade for sapphire substrate, *Sci. Technol. Adv. Mater.* 6 (2005) [120]–[122] <https://doi.org/10.1016/j.stam.2004.11.002>.
- [8] R. Bobbili, V. Madhu, A Modified Johnson-Cook Model for FeCoNiCr high entropy alloy over a wide range of strain rates, *Mater. Lett.* 218 (2018) [103]–[105] <https://doi.org/10.1016/j.matlet.2018.01.163>.
- [9] Yameng Wei, Zhigang Lu, Kehui Hu, et al., Dynamic response of ceramic shell for titanium investment casting under high strain-rate SHPB compression load, *Ceram. Int.* 44 (2018) 11702–11710 <https://doi.org/10.1016/j.ceramint.2018.03.247>.
- [10] G.R. Johnson, W.H. Cook, Fracture characteristics of three metals subjected to various strains, strain rates, temperatures and pressures, *Eng. Fract. Mech.* 21 (1985) 31–48, [https://doi.org/10.1016/0013-7944\(85\)90052-9](https://doi.org/10.1016/0013-7944(85)90052-9).
- [11] F. Gao, J. He, E. Wu, et al., Hardness of covalent crystals, *Phys. Rev. Lett.* 91 (2003) 1–4, <https://doi.org/10.1103/PhysRevLett.91.015502>.
- [12] Lingling Wang, Jun Liang, Guodong Fang, et al., Effects of strain rate and temperature on compressive strength and fragment size of ZrB₂-SiC-graphite composites, *Ceram. Int.* 40 (2014) 5255–5261 <https://doi.org/10.1016/j.ceramint.2013.10.097>.
- [13] Y.F. Zhang, J. Zheng, J.X. Yu, et al., Impact of strain rate on the hardness and elastic modulus of human tooth enamel, *J. Mech. Behav. Biomed. Mater.* 78 (2017)

- 491–495 <https://doi.org/10.1016/j.jmbbm.2017.12.011>.
- [14] Hana Jung, Hoi Kil Choi, et al., High strain rate effects on mechanical properties of inductively coupled plasma treated carbon nanotube reinforced epoxy composites, *J. Compos. Part B* 154 (2018) 209–215 <https://doi.org/10.1016/j.compositesb.2018.08.015>.
- [15] M.M. Chaudhri, J.K. Wells, A. Stephens, Dynamic hardness, deformation and fracture of simple ionic crystals at very high rates of strain, *Philos. Mag. A* 43 (1981) 643–664, <https://doi.org/10.1080/01418618108240400>.
- [16] A. Luke, Hanner John, J. Pittari III, Jeffrey J. Swab, Dynamic hardness of cemented tungsten carbides, *Int. J. Refract. Metals Hard Mater.* 75 (2018) [294]–[298] <https://doi.org/10.1016/j.jjrmhm.2018.05.007>.
- [17] Jitang Fan, Cheng Wang, Dynamic compressive response of a developed polymer composite at different strain rates, *J. Compos. Part B* 152 (2018) [96]–[101] <https://doi.org/10.1016/j.compositesb.2018.06.025>.
- [18] A.H. Almasri, G.Z. Voyiadjis, Effect of strain rate on the dynamic hardness in metals, *J. Eng. Mater. Technol.* 129 (2007) 505–512, <https://doi.org/10.1115/1.2744430>.
- [19] Weiliang zhang, Xinfeng Cheng, et al., Effect of strain rate and temperature on dynamic mechanical behavior and microstructure evolution of ultra-high strength aluminum alloy, *J. Mater. Sci. Eng.* 730 (2018) [336]–[344] <https://doi.org/10.1016/j.msea.2018.06.018>.
- [20] N.J. Edwards, W. Song, S.J. Cimpoeu, et al., Mechanical and microstructural properties of 2024-T351 Aluminium using a hat-shaped specimen at high strain rates, *Mater. Sci. Eng., A* 720 (2018) 203–213 <https://doi.org/10.1016/j.msea.2018.02.049>.
- [21] Akx Malik, Tanusree Chakraborty, et al., Strain rate effect on the mechanical behavior of basalt: observations from static and dynamic tests, *J. Thin-Walled Struct.* 126 (2018) 127–137 <https://doi.org/10.1016/j.tws.2017.10.014>.
- [22] Kun Liu, Zhilin Wu, et al., Strain rate sensitive compressive response of gelatine: experimental and constitutive analysis, *J. Compos.* 64 (2017) [254]–[266] <https://doi.org/10.1016/j.polymertesting.2017.09.008>.
- [23] Jingwei Wang, Tianyu Yu, Ding Wenfeng, et al., Wear evolution and stress distribution of single CBN superabrasive grain in high-speed grinding, *Precis. Eng.* 54 (2018) [70]–[80] <https://doi.org/10.1016/j.precisioneng.2018.05.003>.
- [24] X. Wang, C. Huang, B. Zou, et al., Dynamic behavior and a modified Johnson–Cook constitutive model of Inconel 718 at high strain rate and elevated temperature, *Mater. Sci. Eng.* 580 (2013) 385–390 <https://doi.org/10.1016/j.msea.2013.05.062>.
- [25] J. Sheikh-Ahmad, J. Twomey, ANN constitutive model for high strain-rate deformation of Al 7075-T6, *Mater. Process. Technol.* 186 (2007) [339]–[345] <https://doi.org/10.1016/j.jmatprotec.2006.11.228>.
- [26] Chenwei Dai, Tianyu Yu, et al., Single diamond grain cutting-edges morphology effect on grinding mechanism of Inconel 718, *Precis. Eng.* 55 (2019) [119]–[126] <https://doi.org/10.1016/j.precisioneng.2018.08.017>.
- [27] Nicola Scholl, Florian Minuth-Hadi, Klaus Thiele, Modelling the strain rate dependent hardening of constructional steel using semi-empirical models, *Constr. Steel Res.* 145 (2018) 414–424 <https://doi.org/10.1016/j.jcsr.2018.02.013>.
- [28] Junlei Wei, Genwei wang, et al., Dynamic mechanical properties and constitutive relationship of particle-reinforced AZ91D composites, *Alloy. Comp.* 767 (2018) 210–214 <https://doi.org/10.1016/j.jallcom.2018.06.049>.
- [29] Yancheng Zhang, J.C. Outeiro, Tarek Mabrouki, On the selection of Johnson–Cook constitutive model parameters for Ti-6Al-4V using three types of numerical models of orthogonal cutting, *Thin-Walled Struct.* 31 (2015) 112–117 <https://doi.org/10.1016/j.procir.2015.03.052>.
- [30] M. Tiryakioğlu, On the relationship between Vickers hardness and yield stress in Al-Zn-Mg-Cu alloys, *Mater. Sci. Eng.* 633 (2015) [17]–[19] <https://doi.org/10.1016/j.msea.2015.02.073>.
- [31] Tao Fu, Xianghe Peng, Cheng Huang, et al., Strain rate dependence of tension and compression behavior in nano-polycrystalline vanadium nitride, *Ceram. Int.* 43 (2017) 11635–11641 <https://doi.org/10.1016/j.ceramint.2017.05.342>.
- [32] M.M. Chaudhri, J.K. Wells, A. Stephens, Dynamic hardness, deformation and fracture of simple ionic crystals at very high rates of strain, *Philos. Mag. A* 43 (1981) 643–664 <https://doi.org/10.1080/01418618108240400>.